

Unusual Dielectric Relaxation in Lightly Doped n-Type Rhombohedral BaTi_{0.85}Zr_{0.15}O₃:Ta Ferroelectric Ceramics

Jun Xu and Mitsuru Itoh*

Materials and Structures Laboratory, Tokyo Institute of Technology, 4259 Nagatsuta, Midori,
Yokohama 226-8503, Japan

Abstract

The dielectric properties of tantalum doped BaTi_{0.85}Zr_{0.15}O₃ were investigated. The conventional solid state reaction method was used to make the ceramic samples. The composition was close to the pinch point of the three structure phase transitions in BaTiO₃. Powder X-ray diffraction result indicated that the samples were in very slightly distorted rhombohedral structure at room temperature, and the dielectric measurement showed only cubic-to-rhombohedral phase transition occurred. Instead of a sharp peak characteristic of a ferroelectric (FE) transition, the large dielectric response was similar to those in nonferroelectric perovskites CaCu₃Ti₄O₁₂, AFe_{1/2}B_{1/2}O₃ (A=Ba, Sr, Ca; B=Nb, Ta, Sb) and IBLC (Internal Barrier Layer Capacitance) BaTiO₃ based FE ceramics. However, unlike its FE analogue, the conventional BaTiO₃ based IBLC ceramics, our samples showed weaker temperature dependence of relative permittivity which spans over a wide temperature range. A Maxwell-Wagner type relaxation in the FE state was observed. Moreover, another relaxation mode appears from the vicinity of FE phase transition temperature T_C, and extends over a narrow temperature range, with unusual slowing down of relaxation rate as temperature rises, which is contrary to what is commonly observed. We associate these unusual phenomena with the very slightly distorted rhombohedral structure of our samples and the presence of the grain boundary barrier layer where oxygen vacancies distribute non-homogeneously.

* Corresponding author. Present address: junxu@hiroshima-u.ac.jp

Introduction

Mixed perovskite oxides exhibit a rich variety of dielectric relaxation phenomena at the low and intermediate frequency ranges (≤ 1 MHz). This behavior of the frequency dispersion of dielectric permittivity can occur at very low and very high temperatures, depending on the physical mechanism and the characteristic thermal activation energy. The origins can be both intrinsic (determined mainly by the lattice symmetry) and extrinsic (depending on the microstructures which can be modified by sample processing procedures).

In the well established off-center ion model, relaxation occurs through the hopping of the off-center ions among several equivalent energy minima which are determined by parameters such as the crystal symmetry, external field and the local environment. This type of dipole relaxation is responsible for most of the observed dipole dispersions, such as, in doped quantum ferroelectrics KTaO_3 , SrTiO_3 , etc., as discussed in reference 1.

The hopping of charge carriers (electrons and polarons), is also shown to make much contribution to dielectric response other than conductivity,²⁻³ and may interact with the relaxing species in the lattice, resulting in diffuse dielectric anomalies.² The charge carriers may be from dopant ions and/or oxygen vacancies.

Oxygen vacancy is often unavoidable in perovskite oxides, especially under a high firing temperature and/or low partial oxygen pressure. The contribution of oxygen vacancies to dielectric relaxation can be 3-fold. The first is that oxygen vacancy can hop in the lattice, leading to the associated dipolar moment reorientation, which is in the frame of off-center ion model.⁴ The second is by contributing conducting electrons through ionization. The conducting electrons (or small polarons in some cases), hop from one localized state to another in the lattice, equivalent to the reorientation of effective electric dipoles.^{3,5} The

third is that it can also manifest itself through one type of interfacial polarization mechanism, the dielectric relaxation of which is Maxwell-Wagner (MW) relaxation.⁶ This is realized by different level of oxygen deficiency in different regions within the sample, leading to electric heterogeneity in a crystallographical single phase. The grain boundary in polycrystalline ceramics and various defect structures (such as twin boundary, dislocation) in single crystals play an important role in this mechanism.

The MW effect usually leads to dielectric relaxation with very high dielectric permittivity, and was shown to be the main mechanism in the recently found perovskites $\text{CaCu}_3\text{Ti}_4\text{O}_{12}$ ⁷⁻⁹ (CCTO) and $\text{AFe}_{1/2}\text{B}_{1/2}\text{O}_3$ ($\text{A} = \text{Ba, Sr, Ca}$; $\text{B} = \text{Nb, Ta, Sb}$)¹⁰ (AFBO). Both two are non-ferroelectric and exhibit weak temperature dependent high dielectric permittivity over a wide temperature range which subsequently relax out at low temperatures. The very high dielectric permittivity arises from the same mechanism as in the internal barrier layer capacitor (IBLC) ferroelectric (FE) ceramics, in which the energy barrier at the grain boundary is important. IBLC mechanism has been utilized commercially in mostly BaTiO_3 -based ceramics.¹¹ However, there, the high permittivity in the vicinity of FE phase transition temperature T_C is more governed by FE response and varies more strongly with temperature, comparing to nonferroelectric CCTO and AFBO.

In all the dielectric relaxations described above, the relaxation rate increases as temperature increases, as can be expected from a thermally activated process. We report here an unusual relaxation mode in which the relaxation rate decreases as temperature increases. It was observed in the lightly donor doped rhombohedral FE $\text{Ba}(\text{Ti}_{0.85}\text{Zr}_{0.15})\text{O}_3\text{:Ta}$ ceramics sintered in air, in a narrow temperature range starting from the vicinity of T_C . And the dielectric response of the samples show similar behavior as in CCTO and AFBO, namely, weak temperature dependent high relative permittivity over a wide temperature range which relax out at low temperature, which is a second interesting observation: MW relaxation in

the FE state. We ascribe these unusual phenomena to the very slightly distorted rhombohedral crystal structure of our samples and the presence of grain boundary barrier layers where oxygen vacancies distribute non-homogeneously.

Experimental

The conventional solid state reaction method was used to make the Ta doped $\text{Ba}(\text{Ti}_{0.85}\text{Zr}_{0.15})\text{O}_3$ samples. The nominal composition is $\text{Ba}_{1-0.5x}(\text{Ti}_{0.85}\text{Zr}_{0.15})_{1-x}\text{Ta}_x\text{O}_3$ with $x=0, 0.08\%, 0.2\%$ and 0.5% . Stoichiometric BaCO_3 (99.99%), TiO_2 (99.9%), ZrO_2 (99.99%), Ta_2O_5 (99.9%) were thoroughly mixed in alcohol, calcined in 1250°C – 1300°C with intermediate grindings. Pressed samples in disk shape with 10mm diameter were sintered at 1400°C or 1500°C for 6 hours in air after holding at 500°C for 8 hours to burn out the binder. Finally, the samples were furnace cooled to room temperature.

The phase purity was identified by X-ray diffraction using $\text{Cu K}\alpha$ radiation at 50kV and 300mA with a rotating anode diffractometer M18XHF from MAC Science. Gold electrodes were fired on the polished surfaces of the samples for dielectric measurements. The dielectric permittivity was measured in the temperature range of 5K-400K using a HP4284A LCR meter. To avoid non-linear effect, small probing ac field $\sim 50\text{v/m}$ was used. Resistivity measurement in the same temperature range was carried out using a Physical Property Measurement System from Quantum Design by a standard 4 probe method.

Results and Discussion

The pinch effect for the three phase transitions in BaTiO_3 upon Zr substitution for Ti is well known. The three T_C 's tend to pinch together at certain amount of Zr substitution above which only cubic-rhombohedral phase transition occurs. The composition of our samples is just close to this pinch point in the $\text{Ba}(\text{Ti,Zr})\text{O}_3$ phase diagram.¹² Careful X-ray diffraction measurement at room temperature show our samples are pseudo-cubic with very small rhombohedral distortion. Figure 1 is a result for the 0.08% Ta

doped sample (denoted as BTZ:Ta008 hereafter.), which was taken in a step scan mode with step size 0.02° and counting time 2 seconds. We note that, the split of $\langle hkl \rangle$ reflections is so light that it is not discernible at our routine continuous scan mode for phase identification. The very light split, or more exactly, the appearance of a shoulder, for high angle reflections, such as the characteristic $\langle 222 \rangle$ reflection at around $2\theta \sim 82.7^\circ$, can only be observed at much slower scan speed or step scan mode like (0.02° , 2sec). Apart from the pseudo-cubic peaks, no discernible unindexed peak was observed. Accordingly, dielectric permittivity measurements show only one sharp peak characteristic of FE transition at 343 K for $\text{Ba}(\text{Ti}_{0.85}\text{Zr}_{0.15})\text{O}_3$ sample, confirming that only one cubic-rhombohedral phase transition exists with $T_C = 343$ K for $x=0$.

For the lightly Ta doped samples ($x=0.08\%$, 0.2% , 0.5%), however, the temperature dependent dielectric permittivity ($\epsilon'(T)$) behaves drastically different. Instead of a sharp peak indicative of the FE transition, $\epsilon'(T)$ shows weak temperature dependent permittivity at a high value ($\sim 10^4$) over a wide temperature range from above T_C (see below) to $\sim 100\text{K}$, below which a large drop of two orders of magnitude occurs with large frequency dispersion. A typical result is shown in Figure 2 for BTZ:Ta008. The behavior is very similar to that in CCTO and AFBO, However, compared to those two cases, in our samples, ϵ' varies more with temperature and frequency. In addition, at high frequency, (e.g. 1 MHz), a small peak anomaly at $\sim 340\text{K}$ can be clearly seen, which is the manifestation of the cubic-rhombohedral FE phase transition (see below).

The imaginary part of permittivity ϵ'' shows two peaks with frequency dispersion, indicating two relaxation modes (Figure 2(b)). The low T mode corresponds to the 100-fold sharp drop of $\epsilon'(T)$ step, and the peak shifts to higher temperature with increasing frequency. The high T mode begins to appear

around T_C . Surprisingly, its peak shifts to higher temperature with decreasing frequency, which is contrary to commonly observed dielectric relaxations.

Dielectric relaxation can be more clearly seen from frequency dependent behavior. Figure 3 shows the real part of permittivity as a function of frequency at fixed temperatures. $\epsilon'(f)$ generally shows two plateaus at low and high frequency ranges respectively. The drop from the high plateau to the low one occurs at increasingly lower frequency when the temperature decreases, exhibiting a large frequency dispersion region. In addition, there is a minor intermediate plateau appearing in the $\epsilon'(f)$ curves for temperatures above 330 K, a manifestation of the weak high T mode relaxation process.

Accordingly, the frequency dependent imaginary permittivity $\epsilon''(f)$ shows two distinct behavior at two different temperature regions (Figure 4). At $T < 330\text{K}$, $\epsilon''(f)$ curves show only one distinct peak which shifts to higher frequency with increasing temperature, corresponding to the low T mode in Figure 2. At $T > 330\text{K}$, a second, weaker peak gradually evolves from the high frequency side and migrate to low frequency side with decreasing peak amplitude as temperature increases, which corresponds to the high T mode in Figure 2. Thus, the results show that there is only one relaxation process (low T mode) below 330 K, and two (low T mode + high T mode) above 330 K. The two modes above 330 K can be distinctively decomposed after resolving each set of peaks by curve fitting with two peaks. The relaxation frequency for each mode can thus be clearly extracted, which are plotted in Figure 5.

The low T mode was found to be a Debye-type relaxation process from Cole-Cole plot (not shown here). And the Arrhenius plot in Figure 5 shows that the relaxation rate $\omega (=2\pi f)$ at low temperatures follows the Arrhenius law $\omega = \omega_0 \exp(-\Delta_d/kT)$, with the activation energy $\Delta_d = 0.128\text{eV}$, and the pre-exponential frequency $\omega_0 = 1.9 \times 10^9 \text{Hz}$. The latter value indicates that the relaxation motion of low T mode is not an

ionic process, and is comparable to that reported in CCTO.⁹ Above 200K, the relaxation rate of low T mode deviates from the low temperature Arrhenius fit, which is found to be linked to the overall conductivity behavior (see below). On the other hand, contrary to the low T mode relaxation which spans over a wide temperature range, the high T mode relaxation occurs in a narrow temperature range starting from the vicinity of T_C and exhibits unusual slowing down of the relaxation rate with temperature rising.

We found that the observed dielectric response in lightly doped samples strongly depends on sintering and post-sintering annealing conditions. The color of the sample without Ta doping is light yellow, whereas dark blue-gray for the lightly doped ones indicating a reduced state. If sintering the sample in a small flow of oxygen instead of in air, then we got light yellowish samples with only one sharp ϵ' peak characteristic of FE phase transition, and there is no dielectric relaxation observed. The FE phase transition temperature T_C shows systematic decrease with increasing dopant concentration, indicating the incorporation of Ta dopant into the lattice. The T_C for each lightly doped sample sintered in oxygen flow is coincident with the peak anomaly at high frequencies for the air-sintered samples (see Figure 2), indicating the peak anomaly at high frequencies is due to the FE transition. Annealing the air-sintered samples in a small oxygen flow also tends to diminish the large $\epsilon'(T)$ plateau and the associated frequency dispersion, with increasing FE phase transition feature at high frequencies. The annealing effect is more prominent for higher doped samples, e.g. the 0.5% Ta doped one, but little for the most lightly doped, e.g. BTZ:Ta008. The details will be published elsewhere.

The crucial dependence of the dielectric properties in sintering and post-sintering annealing condition as described above strongly suggests that the observed phenomena, namely, the enhanced large relative permittivity in a wide temperature range with weak temperature dependence, Debye-type relaxation at low temperatures in the FE state, and the unusual slowing down of the relaxation rate with increasing

temperature for the high T mode which occurs in a narrow temperature range starting from the vicinity of T_C , stem from ceramic microstructure which is related to oxygen deficiency. As in CCTO⁷⁻⁸ and AFBO¹⁰, and IBLC BaTiO₃ based FE ceramics¹¹, the observed dielectric response is caused by the formation of boundary barrier layers due to a microstructure consisting of semiconducting grains and insulating grain boundaries. It's known that, semiconducting grains are produced by losing oxygen during sintering at high temperature, and the subsequent cooling process after sintering results in reoxidation along grain boundaries, yielding the insulating nature of grain boundaries. The absorbed oxygen at the grain boundaries are electron traps, or acceptors, which attract conducting electrons from the n-type semiconductive grains, creating a depletion layer with built in energy barrier, in the vicinity of grain boundaries. In BaTiO₃ based FE ceramics, the presence of grain boundary barrier layers results in the well known IBLC effect and PTCR (Positive Temperature Coefficient of Resistivity) effect,¹³⁻¹⁴ which, we believe, is also a key factor underlying the observed unusual dielectric response in our samples.

From semiconductor theory, the width of the depletion layer at the grain boundary is:

$$b = n_s/2n_0 \quad (1)$$

where n_s is the occupied grain boundary acceptor states, and n_0 the free charge carrier density. The height of the potential barrier ϕ which is built in with the depletion layer, is expressed as:

$$\phi = en_s^2/(8\epsilon_r\epsilon_0n_0), \quad (2)$$

where e is the electron charge, ϵ_r the relative permittivity in the grain boundary layer, ϵ_0 the permittivity in vacuum. Both n_s and ϵ_r vary with temperature. In BaTiO₃ based FE ceramics, ϵ_r follows the Curie-Weiss law above T_C . Consequently, the rapid decrease of ϵ_r above T_C leads to a proportionally increased Φ , thus an anomalous increase of resistivity ρ ($\rho \propto \exp(\Phi/kT)$), creating the PTCR effect.

The width of depletion layer, b , is largest at about T_C , where all the surface acceptor states at grain boundaries are occupied. As temperature is increased above T_C , depopulation process of the occupied acceptor states begins to start as the acceptor energy is approaching the Fermi level. As a result, b decreases gradually as n_s decreases. On the other hand, below T_C , the depletion layer will be refilled, more or less, by the charge compensation mechanism due to the incontinuous normal components of the spontaneous polarization at the grain boundary in the FE state. Therefore, b decreases rather sharply as temperature decreases below T_C . Such a variation of the width of depletion layer as a function of temperature in BaTiO₃ ceramics has been experimentally observed.¹⁵

In BaTiO₃ based high permittivity IBLC ceramics, below T_C , due to the charge compensation mechanism, the high capacitance depletion layer is more or less diminished, thus making ineffective, more or less, of an equivalent circuit of parallel capacitors. Consequently, the relative permittivity below T_C is more governed by ferroelectric response, yielding a quite strong temperature dependent behavior. On the other hand, such an equivalent circuit will not be destroyed in the nonferroelectric perovskites CCTO and AFBO, where, the large relative permittivity persists with weak temperature dependence over a wide temperature range, until finally relax out at low temperature due to the MW relaxation which just originates from the effective serial-parallel circuit of the distinct grain and grain boundary barrier layer effects.⁶

The survival of the effective circuit in the FE state in our Ba(Ti_{0.85}Zr_{0.15})O₃:Ta ceramic samples, stems from its pseudo-cubic structure with very light rhombohedral distortion. The previous work in the literature concerned about the cubic-tetragonal FE phase transition in BaTiO₃ based ceramics. The appearance of large spontaneous polarization below cubic-tetragonal FE transition makes the charge compensation mechanism below T_C more effective. On the other hand, as our x-ray data indicates, the rhombohedral distortion of our samples is very small, which means small ionic displacement from the

centric position in the lattice. Hence, the cubic-rhombohedral FE transition in our samples is associated with a much lower spontaneous polarization value, which therefore is less effective to diminish the grain boundary barrier layers. Such a degradation of ferroelectricity in this doping level of Ba(Ti,Zr)O₃ rhombohedral phase can also manifest itself directly in the electric polarization behavior¹². The observed phenomena in our study, i.e., the MW relaxation in the FE state, the weak temperature dependence (or, lack of feature) of the permittivity when passing T_C, are manifestation of the effective circuit in the FE state as in nonferroelectric CCTO and AFBO.

However, as our samples being ferroelectric, there still exist some features in the dielectric response which are different from the nonferroelectric counterparts. For example, the $\epsilon'(T)$ curves show comparatively more temperature dependence below T_C and are more frequency dependent (Figure 2). With decreasing temperature, the magnitude of the high plateaus at low frequency side which is related to boundary layer property, doesn't remain nearly constant as observed in CCTO,⁸⁻⁹ instead, shows a decrease, indicating the existence of charge compensation mechanism (Figure 3).

The low T mode relaxation arises from MW effect due to the effective circuit. The relaxation rate behavior (Figure 5) is found to be closely linked to the overall conductivity behavior which is shown in Figure 6. The strong upturn of the resistivity at around T_C confirms the PTCR effect. Below T_C, it shows semiconductive behavior. At low temperatures, the resistance increases sharply and is beyond the measurable range below 120K. Below ~210 K, it shows a thermally activated conductivity process which follows the Arrhenius law $\rho = \rho_0 \exp(\Delta_r/kT)$ with the activation energy $\Delta_r = 0.125\text{eV}$. The value is close to the one ($\Delta_d = 0.128\text{eV}$) for the low T mode relaxation at the same temperature range, indicating the close relationship between the low T mode relaxation and the conducting behavior in the grain. Above ~210 K, the resistivity behavior deviates from the Arrhenius law, which probably arises from the

growing contribution from the grain boundary layer resistance. The deviation at ~210 K may be due to a critical change of the relative contribution of grain and grain boundary barrier layer. It is interesting to note that in the rhombohedral phase of Nb-doped BaTiO₃ single crystal, a slowing down of the relaxation motion at low temperatures which follows the Arrhenius law was also observed.²

Now let's turn to the high T mode relaxation (Figure 5). First we would note that in pure and doped BaTiO₃, a high frequency polar relaxation mode has been observed in the vicinity of T_C, with relaxation rate being minimum at T_C.^{2,16} This was ascribed to the presence of order-disorder character in the usually accepted displacive picture for the FE phase transition in BaTiO₃. This type of local polar cluster (made up of off center Ti⁴⁺ ions) induced relaxation mode occurs at very high frequencies (> 10⁶ Hz), and the relaxation rate above T_C increases as temperature increases, which obviously is not responsible for the high T mode in our samples. Alternatively, we would relate it to the depletion layer in the FE ceramic samples.

The depletion layer at the grain boundary has been treated as a thin 2D layer. However, it should not always be true. As described above, the width of the depletion layer *b* is the largest at around T_C, and decrease gradually above T_C resulting from the depopulation process of the occupied acceptor states at grain boundary, while decreasing sharply just below T_C due to the charge compensation mechanism of FE phase transition. Experimental results have shown that in the vicinity of T_C, *b* is on the order of tenth of μm.¹⁵ The typical grain size is on the order of μm. Taking into account of the fact that there are double depletion layers at both sides of a single grain boundary, it seems that in some cases, if not in all, the volume effect of the depletion layer area could not be ignored. The study of the dielectric property of the depletion layer in BaTiO₃ ceramics revealed that its equivalent dielectric constant (averaged value over the depletion layer) behaves similarly to that of the grain, namely a Curie-Weiss behavior above T_C which is shifted 11 K downward relative to that of the grain.¹⁷ From the temperature range in which the

high T mode relaxation occurs, and the weaker and declining features of the magnitude, we would suggest that the high T mode arises from the depletion layer.

In our picture, we propose that the ionized oxygen vacancies do not distribute randomly in the depletion layer. The closer it is to the grain boundary, the less there are charged oxygen vacancies. This is very likely, due to two reasons. One, during the reoxidation along the grain boundary in the cooling process, some diffusion of the absorbed oxygen atoms from the grain boundary toward grain interior could happen. Two, the increasing height of the potential barrier when closer to the grain boundary, makes such a distribution of positively charged oxygen vacancies favorable in energy. It is thus expected that the distribution depends on the width of the depletion layer and the associated potential barrier. In such a picture, the slowing down of the relaxation rate of the high T mode with increasing temperature above T_C can be understood as a result from the redistribution of the ionized oxygen vacancies in the depletion layer area when its width decreases with simultaneous change of the potential barrier height. Such a redistribution of the charges may enhance the local potential around the relaxing polar clusters which consist of off center Ti^{4+} ions, due to Coulomb interaction. As a consequence, the relaxation motion slows down. And the gradual shrinkage of the depletion layer area above T_C results in the declining of the amplitude of the high T mode relaxation.

Conclusions

To sum up, we observed, in lightly doped n-type $BaTi_{0.85}Zr_{0.15}O_3:Ta$ FE ceramics, a large relative permittivity spanning over a wide temperature range with weak temperature dependence, which finally relaxes out at low temperatures by a MW effect. The large dielectric response is caused by ceramic microstructures that consist of semiconductive grains and insulating grain boundaries, the same as in nonferroelectric perovskites CCTO, AFBO and ferroelectric $BaTiO_3$ based IBLC ceramics. However, the weaker temperature dependence and wider spanning temperature range, as well as the MW

relaxation, differ from the conventional IBLC BaTiO₃ based ceramics. Moreover, another, and unusual, relaxation mode with slowed down relaxation rate as temperature rises, appears in the vicinity of T_C and extends over a narrow temperature range. We suggest that these unusual phenomena can be understood as effects from the oxygen depletion layer at the grain boundary, in which the very slightly distorted rhombohedral crystal structure plays an important role. The unusual relaxation mode in the vicinity of T_C is attributed to be from the volume effect of the depletion layer area which becomes unignorable when the PTCR effect takes place at FE phase transition, and the slowing down of the relaxation rate with increasing temperature is a consequence of redistribution of charged oxygen vacancies in the depletion layers.

Acknowledgement Part of this work was supported by the 21st century COE program ‘Nanomaterial Frontier Cultivation for Industrial Collaboration’ of the Ministry of Education, Culture, Sports, Science and Technology of Japan.

References

- (1) Samara, G. A. *J. Phys.: Condens. Matter* **2003**, *15*, R367
- (2) Maglione, M.; Belkaoumi, M. *Phys. Rev. B* **1992**, *45*, 2029
- (3) Bidault, O.; Maglione, M.; Actis, M.; Kchikech, M.; Salce, B. *Phys. Rev. B* **1995**, *52*, 4191
- (4) Samara, G. A.; Boatner, L. A. *Phys. Rev. B* **2000**, *61*, 3889
- (5) Chen Ang; Zhi Yu; Cross, L. E. *Phys. Rev. B* **2000**, *62*, 228
- (6) Ion Bunget; Mihai Popescu, *Physics of Solid Dielectrics*, Elsevier, **1978**
- (7) Subramanian, M. A.; Li, D.; Duan, N.; Reisner, B. A.; Sleight, A. W. *J. Solid State Chem.* **2000**, *151*, 323
- (8) Sinclair, D. C.; Adams, T.; Morrison, F.; West, A. R. *Appl. Phys. Lett.* **2002**, *80*, 2153
- (9) Homes, C. C.; Vogt, T.; Shapiro, S.; Wakimoto, S.; Ramirez, A. P. *Science*, **2001**, *293*, 673
- (10) Raevski, I. P.; Prosandeev, S.; Bogatin, A.; Malitskaya, M.; Jastrabik, L. *J. Appl. Phys.* **2003**, *93*, 4130
- (11) Cheng-Fu Yang. *Jpn. J. Appl. Phys.* **1996**, *35*, 1806
- (12) Zhi Yu; Chen Ang; Ruyan Guo; Bhalla, A.S. *J. Appl. Phys.* **2002**, *92*, 1489
- (13) Heywang, W. *Solid-State Electron.* **1961**, *3*, 51
- (14) Jonker, G. H. *Solid-State Electron.* **1964**, *7*, 895
- (15) Da Yu Wang; Kazumasa Umeya. *J. Am. Ceram. Soc.* **1990**, *73*, 669
- (16) Maglione, M.; Boehmer, R.; Loidl, A.; Hoechli, U. T. *Phys. Rev. B* **1989**, *40*, 11441
- (17) Da Yu Wang; Kazumasa Umeya. *J. Am. Ceram. Soc.* **1990**, *73*, 1574

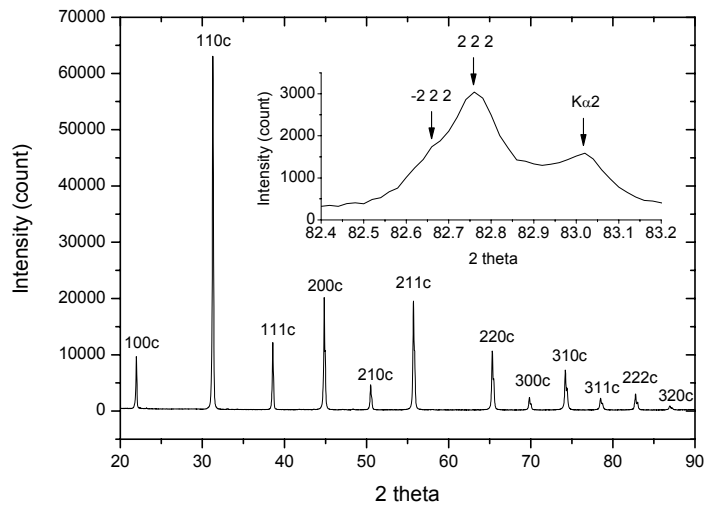


Figure 1. X-ray diffraction pattern recorded at room temperature for the sample BTZ:Ta008 (see text).

The peaks are indexed in a pseudo-cubic structure. Inset: a magnification around 222c peak.

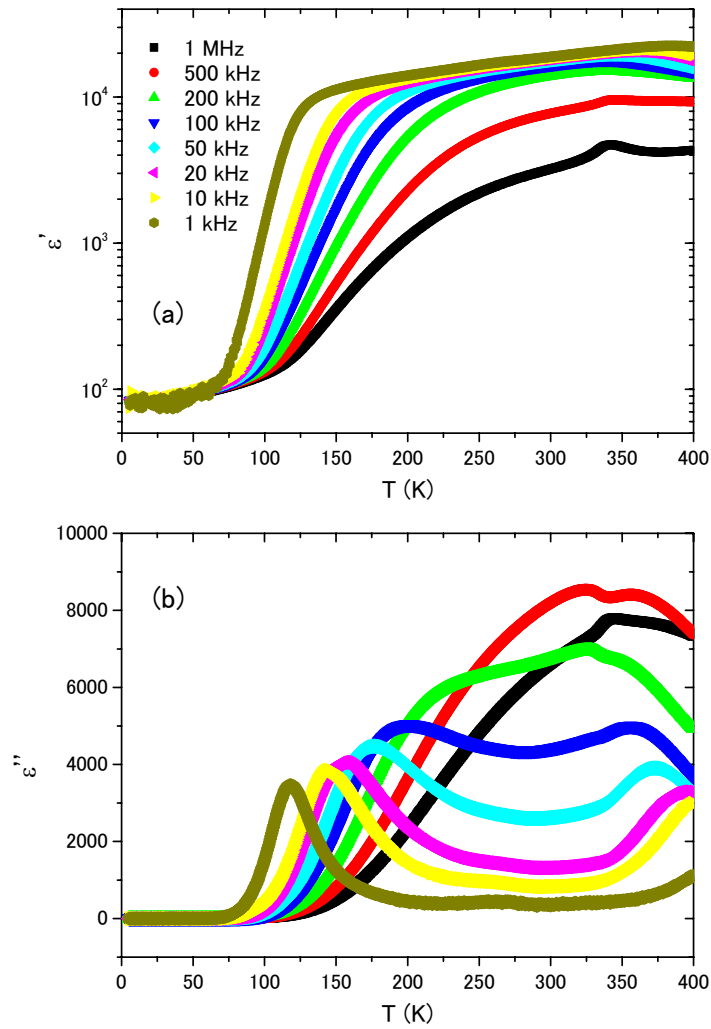


Figure 2. Temperature dependence of dielectric permittivity for BTZ:Ta008.

(a) real part ϵ' , (b) imaginary part ϵ'' .

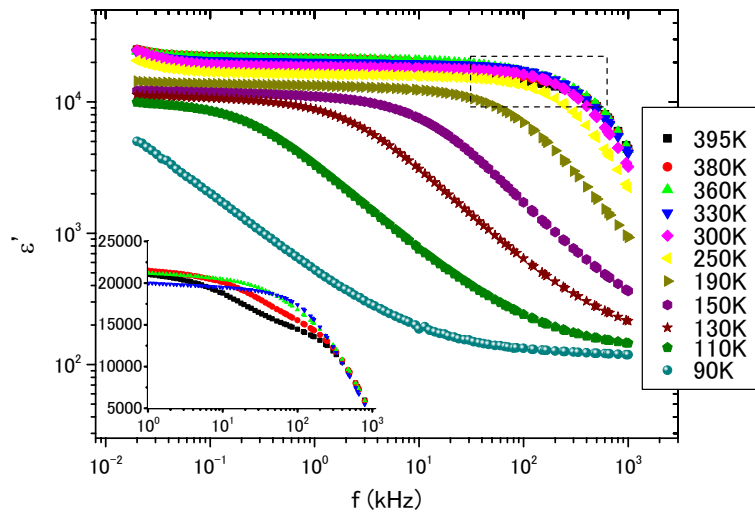


Figure 3. Frequency dependence of ε'' at various temperatures. Inset: Expanded view of the marked area, highlighting the intermediate $\varepsilon''(f)$ plateau for temperatures above 330K.

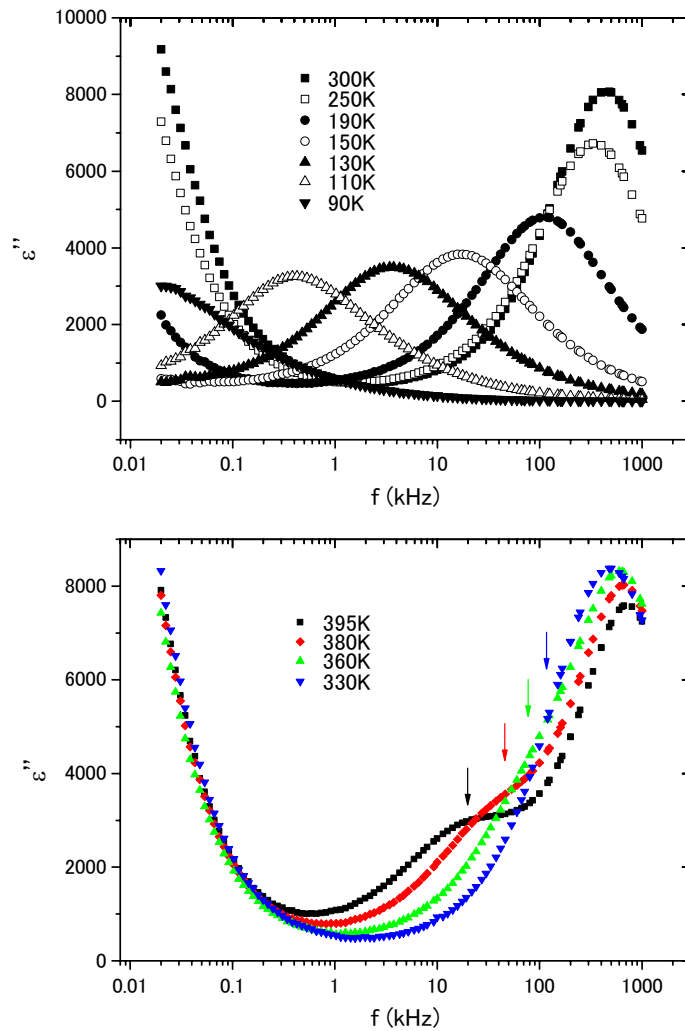


Figure 4. Frequency dependence of ϵ'' at various temperatures. (a) $T < 330\text{K}$, (b) $T \geq 330\text{K}$. The arrows in (b) point to the weak peaks corresponding to the high T mode.

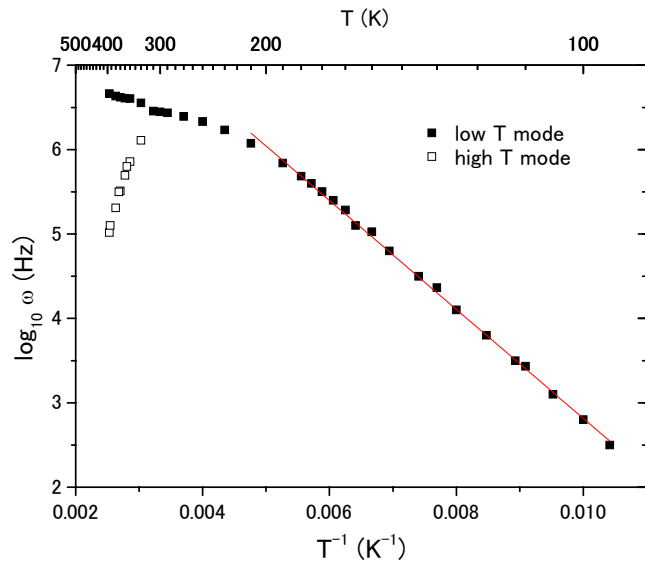


Figure 5. Arrhenius plot of relaxation rate ω versus T^{-1} .

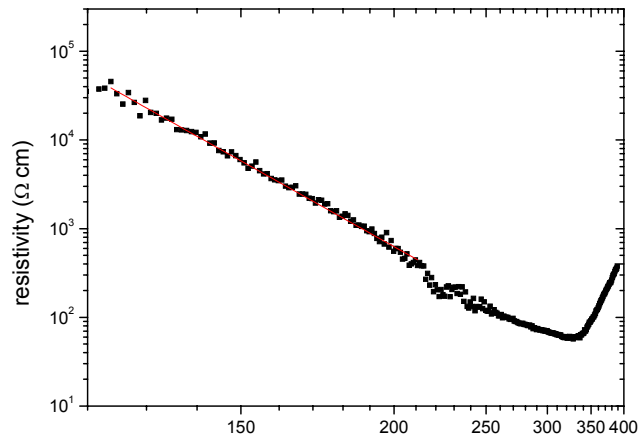


Figure 6. Temperature dependence of dc resistivity in a log-reciprocal plot.